On the computation of slow manifolds in chemical kinetics via optimization and their use as reduced models in reactive flow systems

A. Dedner[§], M. Fein[*], R. Klöfkorn[‡], D. Kröner[‡], D. Lebiedz[*‡], J. Siehr[†], J. Unger[*]
[*]Center for Systems Biology (ZBSA), University of Freiburg, Germany
[†]Interdisciplinary Center for Scientific Computing (IWR), University of Heidelberg, Germany
[‡]Section of Applied Mathematics (AAM), University of Freiburg, Germany
[§]Warwick Mathematics Institute (WMI), University of Warwick, England

***Abstract*— In reaction systems involving different time scales, manifolds of slow motion can be identified. These manifolds can be used for model reduction purposes. We discuss a method based on optimization for the approximation of such manifolds and their use in reactive flow simulations.**

I. Introduction

The mathematical modeling of chemically reactive flows is a complex interplay between flow (convection), diffusive transport, and chemical (combustion) reaction processes, especially if it is based on a detailed combustion mechanism involving a large number of chemical species and reactions. Then complexity reduction and multi-scale approaches show their benefits.

The aim of many model reduction methods is the identification of so-called slow invariant (attractive) manifolds (SIM). In phase space reaction trajectories relax onto these manifolds. Therefore, the dynamics of the full system may be approximated by the dynamics on the SIM.

Many model reduction methods are applied to the chemical source of the equation system, i.e. the reduction operates only on a system of ordinary differential equations (ODE). The results may be tabulated or computed in situ for being included in a simulation of the full system of partial differential equations (PDE), which is solved only for a small number of "represented species".

In this talk we present a method based on optimization of trajectories yielding approximations of slow manifolds. Applications of this method to different mechanisms are shown. The results are used in a simulation of a reactive flow in context of a test mechanism.

II. Slow manifold computation

As common in methods allowing for *species reconstruction*, manifolds are parametrized by so-called reaction progress variables, which are chosen from the whole composition. The method itself is a rule for computing the values of the remaining species if the values of the reaction progress variables is known.

A. Methodology

The dynamical system considered here represents a homogeneous mixture of n_s chemical species and may be formulated as the set of differential equations

$$\begin{aligned} \mathrm{d}_t\phi(t) &= S^\phi(\phi(t),T(t)) \\ \mathrm{d}_t T(t) &= S^T(\phi(t),T(t)) \end{aligned} \tag{1}$$

with the variable $\phi(t) = (\phi_i(t))_{i=1}^{n_\mathrm{s}}$ denoting the state vector at time t. The composition $\phi(t)$, representing the chemical species, is given in units of specific moles; T represents the temperature. The operator d_t represents the total derivative with respect to the free variable t. The source term due to chemical reaction is formulated as S^ϕ and the heat of the reaction is the right hand side S^T for the temperature. It is zero in the isothermal case and guarantees energy conservation in the adiabatic case.

Previously, see e.g. [1], [2], we presented a method for approximating a SIM located in the phase space, the range space of solutions of an ODE system. Our method is based on optimization. The main problem to be solved may be formulated as

$$\min_{\phi,T} \int_{t_0}^{t_\mathrm{f}} \Phi\left(\phi(t)\right)\ \mathrm{d}t \tag{2a}$$

subject to

$$\mathrm{d}_t\phi(t) = S^\phi(\phi(t),T(t)) \tag{2b}$$
$$\mathrm{d}_t T(t) = S^T(\phi(t),T(t)) \tag{2c}$$
$$0 = C(\phi(t_*),T(t_*)) \tag{2d}$$
$$\phi_j(t_*) = \phi_j^{t_*}, \quad j \in \mathcal{I}_\mathrm{rpv} \tag{2e}$$
$$t_0 \leqslant t_* \leqslant t_\mathrm{f} \quad \text{(fixed)} \tag{2f}$$

The system's dynamics enter the optimization problem as equality constraints. Non-differential constraints are collected in the function C in (2d). On the one hand it represents the conservation of element mass in the system and on the other hand it includes the conservation of energy or temperature in the adiabatic and isothermal case, resp. This has to be required explicitly as it is fulfilled for any initial condition of the ODE system (1). The index set $\mathcal{I}_\mathrm{rpv}$ contains the indices of the reaction progress variables which have fixed values at time t_*. These variables parametrize the SIM. The objective function is defined in (2a) where $\Phi\left(\phi(t)\right)$ is used. It is the optimization criterion related to the degree of relaxation

of chemical forces. In the following the optimization criterion

$$\Phi\left(\phi(t)\right) = \|J_{S^\phi}\ S^\phi\|_2^2 \tag{3}$$

is used, where J_{S^ϕ} is the Jacobian of S^ϕ. The idea behind is to exploit a property of the trajectories which is minimal for slow trajectories. The term $\mathrm{d}_{tt}\phi = J_{S^\phi}\ S^\phi$ (being the second derivative of the state vector at time t) has similarity to acceleration, hence the integral in the objective function is similar to the mean velocity.

The slow manifold is appoximated by the state $\phi(t)$ of the system at a certain point in time in the interval $[t_0, t_\mathrm{f}]$, where the ODE (2b, 2c) is solved. This point in time is called t_*. Good results can be achieved for $t_* = t_\mathrm{f}$, clarifying the inequality (2f). This means the dynamics of the system along a certain time $t_\mathrm{f} - t_0$ which lead the system to a final state fulfilling all necessary conservation relations and the values of the reaction progress variables to the desired value $\phi_j^{t_*}$ under a minimal value of (2a) determines the value of the non-fixed states.

B. Theoretical results

Due to mass conservation and positivity of the species' values the realizable reaction space is effectively a polytope, a compact subset of the phase space. Using a sufficiently smooth objective function in the optimization problem (2) always guarantees the existence of a solution of the problem, see [3].

Furthermore the criterion (3) allows for further theoretical results. In test cases where the dynamical system – here the ODE system (1) – has an analytical solution, the optimality conditions can also be evaluated analytically. This is the case e.g. for a linear ODE system and the Davis–Skodje test problem [4]

$$\begin{aligned} \mathrm{d}_t y_1 &= -y_1 \\ \mathrm{d}_t y_2 &= -\gamma y_2 + \frac{(\gamma-1)y_1 + \gamma y_1^2}{(1+y_1)^2}, \end{aligned} \tag{4}$$

where $\gamma > 1$ is a measure for the spectral gap (stiffness) of the system. This model has also an analytical SIM in the phase space, where solution trajectories are attracted to. This means an estimate of the error of the method can be given. We have shown for a two-dimensional linear system and the Davis–Skodje problem (4) that our method identifies the correct SIM for an infinite time horizon, i.e. in the limit $t_0 \to -\infty$ [3].

C. Numerical results

For solving the optimization problem numerically, two different approaches for discretization are used. On the one hand a single shooting approach is used which benefits from a small system of optimality conditions. On the other hand a collocation approach (a complete discretization of states in time) results in better stability properties of the algorithm.

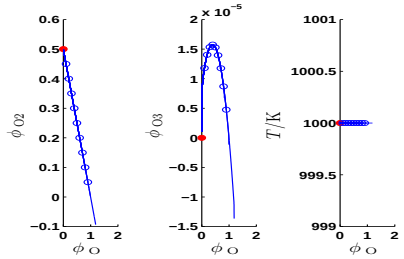

Fig. 1. Plot of the solution of the optimization problem for the ozone decomposition mechanism at a fixed temperature of $T = 1000$ K at a fixed volume $V = 1.0$ m^3. The value of ϕ_O is chosen as progress variable in mol/kg. The solutions of the optimization problem are shown as blue rings. Trajectories emanating of those are also shown as they converge to equilibrium (red dot on the left of the subplots).

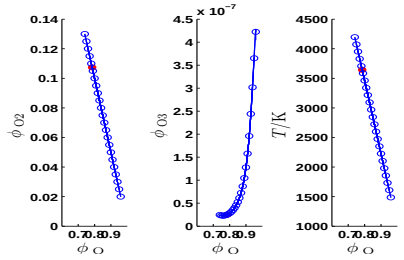

Fig. 2. Plot of the solution of the ozone decomposition mechanism at a fixed pressure $p = 8500$ Pa and a fixed enthalpy corresponding to a system consisting only of $\phi_\mathrm{O} = 1.0$ mol/kg at $T = 1000$ K.

Results for an ozone decomposition mechanism: In the following results for an ozone decomposition mechanism are shown. The mechanism consists of three components: O, O_2, and O_3. The Arrhenius parameters can be found in [5]. For the heat of the reaction appropriate thermodynamic data is used. The results are obtained under isothermal and isochoric (Fig. 1), isothermal and isobaric (not shown), adiabatic and isochoric (not shown), and adiabatic and isobaric (Fig. 2) conditions, resp.

It can be seen in the figures, that the method identifies a manifold having only a small lack of invariance.

III. Computing the tangent space

For using the computed slow manifold a projection to the tangent space of the manifold has to be performed. Hence the tangent vectors of the manifold in any point of the manifold are needed. Consider again the basic optimization problem (2). If we consider the fixed value(s) $\phi_j^{t_*}$ as parameters $\bar{r} = \phi_j^{t_*}$ in the optimization, parameter sensitivities, see [6], can be computed as

$$\begin{bmatrix} \nabla_{\phi,\phi}\mathcal{L}(\phi^*,\lambda^*,\bar{r}) & \nabla_\phi G(\phi^*,\bar{r}) \\ \nabla_\phi G^\mathrm{T}(\phi^*,\bar{r}) & 0 \end{bmatrix} \begin{bmatrix} \frac{\mathrm{d}\phi^*}{\mathrm{d}r}(\bar{r}) \\ \frac{\mathrm{d}\lambda^*}{\mathrm{d}r}(\bar{r}) \end{bmatrix} = - \begin{bmatrix} \nabla_{\phi,r}\mathcal{L}(\phi^*,\lambda^*,\bar{r}) \\ \nabla_r G(\phi^*,\bar{r}) \end{bmatrix} \tag{5}$$

where

$$\nabla_{\phi,r}\mathcal{L}(\phi^*,\lambda^*,\bar{r}) = \nabla_{\phi,r}[\mathrm{obj}] + \lambda^{*,\mathrm{T}}\nabla_{\phi,r}G(\phi,\bar{r}) = 0$$

are derivatives of the Lagrangian function $\mathcal{L}$ and all equality constraints (maybe also resulting from discretization) are assembled in the function G. The objective function is abbreviated with [obj]. The Lagrange multipliers in the solution are denoted by λ^*. The matrix on the very left in Eq. (5) is the KKT-matrix used in the optimization. The right hand side in Eq. (5) is sparse since it is linear in r or does not depend on r at all. In case of an explicitly demanded positivity of species and temperature a similar formula applies.

The resulting matrix of manifold tangent vectors $\frac{\mathrm{d}\phi^*(t_*)}{\mathrm{d}r}(\bar{r})$ can be used for a numerical continuation strategy, if a family of parametric optimization problems is solved for tabulating the manifold. It is also used in the following for computing the normal space of the manifold.

IV. Coupling detailed chemical kinetics to physical transport

A. Theory

When physical transport processes such as convection and diffusion are present, there is no guarantee that the chemical composition still lies on the SIM.
To see this, consider the following abstract description of an evolution equation involving physical transport

$$\partial_t \zeta = \underbrace{f(\zeta)}_{\text{Chemistry}} + \underbrace{\Psi\left(\zeta, \partial_x\zeta, \partial_x^2\zeta\right)}_{\text{Physical Transport}}.$$

Here, $\zeta \equiv \zeta(x,t,h,T,\rho,\rho E,\ldots,y(x,t))$ denotes the general state variable comprising the species' specific moles, the mixture density, the internal energy, temperature and so forth.
In order to keep notation simple, we confine ourselves to the scalar 1D convection equation and the 1D scalar diffusion equation with constant convection and diffusion, respectively

$$\begin{aligned}\partial_t\zeta(y(x,t)) &= v\partial_x\zeta(y(x,t))\\ \partial_t\zeta(y(x,t)) &= \mathscr{D}\partial_x^2\zeta(y(x,t)).\end{aligned}$$

Thus, using the chain rule and by denoting $y(x,t) \equiv y$ we arrive at

$$\partial_t\zeta(y) = v\partial_x\zeta(y) = v\partial_y\zeta\partial_x y \quad (6)$$
$$\partial_t\zeta(y) = \mathscr{D}\partial_x^2\zeta(y) = \mathscr{D}(\partial_y\zeta\partial_x^2 y + \partial_y^2\zeta(\partial_x y)^2). \quad (7)$$

It is evident from (6) that $\partial_t\zeta$ is a linear combination of $\partial_y\zeta$ and is therefore tangential to the manifold (i.e. it lies in the tangent space of the manifold) whereas only the first part of the right hand side of the diffusion equation lies in the tangent space and the second not.
This accounts for the drawn-off effects of the composition as soon as diffusive processes are involved, cf. fig. 3.

In the remainder of this section we consider isothermal convection-diffusion-reaction equations $y_i \equiv y_i(x,t) : \mathbb{R}^d \supset \Omega \times [t_0, t_\mathrm{f}] \to \mathbb{R}$ with velocities $v_i \equiv v_i(x,t) \in \mathbb{R}^d$ and diffusion coefficients $\mathscr{D}_i(y_i) \in \mathbb{R}$ of the form

$$\partial_t y_i + v_i \cdot \nabla y_i = \nabla \cdot (\mathscr{D}_i(y_i)\nabla y_i) + f_i(y_i) \quad (8)$$

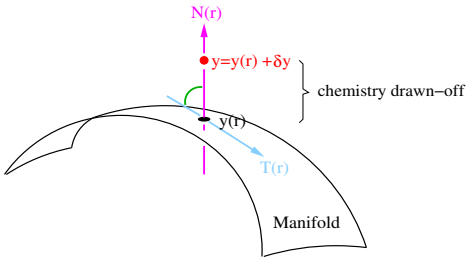

Fig. 3. A graphical representation of the effects caused by diffusion. $N(r)$ and $T(r)$ represent the normal and tangent space of the manifold, respectively.

which make up an n_s-dimensional system

$$\partial_t y + \underbrace{\mathcal{C}\{y\}}_{\text{convection}} = \underbrace{\mathcal{D}\{y\}}_{\text{nonlinear diffusion}} + \underbrace{f(y).}_{\text{chemical source}} \quad (9)$$

Furthermore, we assume that the initial and boundary conditions are on the manifold.

B. The Close-Parallel Assumption

To face the above mentioned drawn-off effects when diffusion comes into play, the *Close-Parallel Assumption* (CPA) has been devised (see [7], [8]) i.e. *aberrations/perturbations caused by diffusion draw the composition onto a manifold which is close and "parallel" to the chemistry based manifold*, cf. fig. 3. Hence, the composition can now be expressed in terms of $r \equiv r(x,t)$, $r \in \mathbb{R}^{n_\mathrm{r}}$, with $n_\mathrm{r} < n_\mathrm{s}$ being the number of reaction progress variables, as

$$y = y^{\mathcal{M}}(r) + \delta y(r),$$

where $y^{\mathcal{M}}(r)$ denotes the point on the manifold $\mathcal{M}$, $\delta y(r)$ is the aberration due to diffusion and $r = B^\mathrm{T} y$ is the reduced description of y, and B^T a user-specified constant matrix (e.g. $B^\mathrm{T} \in \{0,1\}^{n_\mathrm{r}\times n_\mathrm{s}}$). Note that due to the fact that $\delta y(r)$ resides in the unrepresented subspace U, i.e. the subspace spanned by the non reaction progress variables, it can be expressed via $\delta y = U\delta u$.
Upon premultiplying (9) with B^T, applying the CPA and taking advantage of the presumption that the source term, f, is at least once continuously differentiable, and hence Taylor's theorem is applicable, i.e. $f(y^{\mathcal{M}}(r) + U\delta u) \approx f(y^{\mathcal{M}}(r)) + Df(y^{\mathcal{M}}(r))U\delta u$, we get

$$\begin{aligned}&\partial_t r + \mathcal{C}\{r\} = B^\mathrm{T}[\mathcal{D}\{y^{\mathcal{M}}(r)\}\\ &+ f(y^{\mathcal{M}}(r)) + Df(y^{\mathcal{M}}(r))U\delta u].\end{aligned}$$

It should be stressed out that δu is the solution of a generally overdetermined, yet rank-deficient, linear system

$$N^\mathrm{T} Df(y^{\mathcal{M}}(r))U\delta u = -N^\mathrm{T}\mathcal{D}\{y^{\mathcal{M}}(r)\} - N^\mathrm{T} f(y^{\mathcal{M}}(r))$$

since the conservation of mass leads to $\det(Df) = 0$.
For a detailed discussion of the CPA, consult [7], [8].

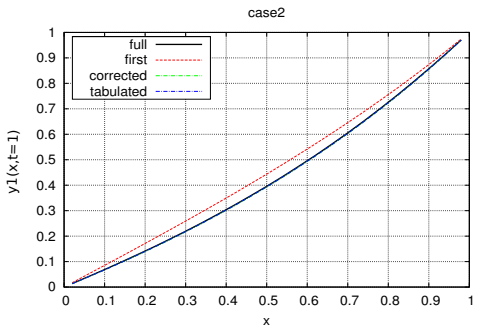

Fig. 4. Result for $a = b = c = d = 1, e = 0, \epsilon = 0.01$. The black curve corresponds to the full model (10), the red dashed curve describes only the evolution of the first equation of (10) (this so-called "first approximation" does not take the drawn-off effects into account) and the blue dashed one describes the CPA approach with calculated SIM data by the above mentioned method.

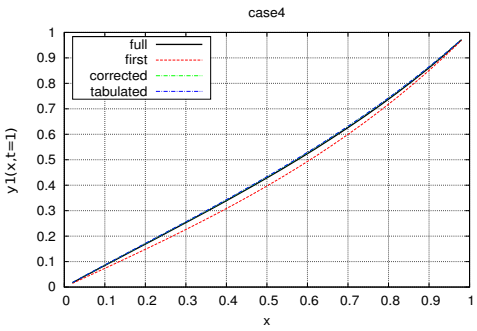

Fig. 5. Result for $a = b = c = 1, d = 2, e = 3, \epsilon = 0.01$. For any explanation see fig. 4.

C. Numerical results for an extended Davis–Skodje mechanism

The CPA has been implemented as C++ interface within the freely available DUNE and DUNE-FEM environment, cf. [9], [10], [11]. The latter contains efficient implementations of *Discontinuous Galerkin* (DG) methods for the discretization of systems such as (9). A detailed exposition of stable DG methods can be found in [12].

We checked our implementation with a toy example given in [7], the so-called *Extended Davis–Skodje mechanism* defined in $[0,1] =: \Omega \times I := [0,1]$

$$\begin{aligned} \partial_t y_1 &= \frac{c}{\epsilon}\left(y_2 - \frac{y_1}{1+ay_1}\right) - dy_1 + \partial_x\left(\mathscr{D}_1 \partial_x y_1\right) \\ \partial_t y_2 &= -\frac{1}{\epsilon}\left(y_2 - \frac{y_1}{1+ay_1}\right) - \frac{y_1}{(1+by_1)^2} \\ &\quad + \partial_x\left(\mathscr{D}_2(x)\partial_x y_2\right), \end{aligned} \tag{10}$$

where $\mathscr{D}_2(x) = \mathscr{D}_1 + e \cdot x, x \in \Omega, a, b, c, d, e \in \mathbb{N}, \epsilon > 0$. The initial and boundary conditions are taken to lie on the (analytical) manifold

$$y = y^{\mathcal{M}}(y_1) = [y_1, y_2]^{\mathrm{T}} = \left[y_1, \frac{y_1}{1+ay_1}\right]^{\mathrm{T}}, \tag{11}$$

namely

$$\begin{aligned} y(x, t=0) &= \begin{bmatrix} x \\ \frac{y_1}{1+ay_1} \end{bmatrix}, \\ y(x=0,t) &= \begin{bmatrix} 0 \\ 0 \end{bmatrix}, y(x=1,t) = \begin{bmatrix} 1 \\ \frac{1}{1+a} \end{bmatrix}. \end{aligned}$$

Instead of using the exact manifold (11), the manifold has been computed numerically via the approach described in the preceding sections.

We only consider the more interesting cases where the SIM is non-linear, i.e. $a \neq 0$ in (11).

These results, see fig. 4, 5, agree quite well with those produced fully analytically in [7, case 2 and case 4].

However, if convection is much larger than diffusion, the latter one will be increased and the composition is drawn off too far from the manifold. In that case, the CPA cannot be applied any more to yield meaningful results (see [7] for discussion).

ACKNOWLEDGMENT

The authors acknowledge support by the DFG through SFB 568 and by the Baden-Württemberg Stiftung.

REFERENCES

[1] D. Lebiedz, "Computing minimal entropy production trajectories: An approach to model reduction in chemical kinetics," *J. Chem. Phys.*, vol. 120, pp. 6890–6897, 2004.
[2] D. Lebiedz, V. Reinhardt, and J. Siehr, "Minimal curvature trajectories: Riemannian geometry concepts for slow manifold computation in chemical kinetics," *J. Comput. Phys.*, vol. 229, pp. 6512–6533, 2010
[3] D. Lebiedz, J. Siehr, and J. Unger, "A variational principle for computing slow invariant manifolds in dissipative dynamical systems," *SIAM J. Sci. Comp.*, accepted, 2011.
[4] M.J. Davis and R.T. Skodje, "Geometric investigation of low-dimensional manifolds in systems approaching equilibrium," *J. Chem. Phys.*, vol. 111, pp. 859–874, 1999.
[5] U. Maas and J. Warnatz, "Simulation of Thermal Ignition Processes in Two-Dimensional Geometries," *Z. Phys. Chem. NF*, vol. 161, pp. 61–81, 1989.
[6] C. Büskens and H. Maurer, "Sensitivity analysis and real-time optimization of parametric nonlinear programming problems," Chap. 1 in "Online Optimization of Large Scale Systems," M. Grötschel, S.O. Krumke, and J. Rambau, Eds., Berlin: Springer, 2001
[7] Z. Ren and S.B. Pope, "The use of slow manifolds in reactive flows," *Comb. Flame*, vol. 147, pp. 243–261, 2006.
[8] Z. Ren and S.B. Pope, "Transport-chemistry coupling in the reduced description of reactive flows," *Comb. Theory Model.*, vol. 11, pp. 715–739, 2007.
[9] DUNE website. *Distributed and Unified Numerics Environment (DUNE)*. URL: http://www.dune-project.org.
[10] DUNE-FEM website. URL: http://dune.mathematik.uni-freiburg.de.
[11] A. Dedner, R. Klöfkorn, M. Nolte and M. Ohlberger, "A generic interface for parallel and adaptive scientific computing: Abstraction principles and the DUNE-FEM module," Comput., vol. 89, 2010.
[12] S. Brdar, A. Dedner and R. Klöfkorn, "Compact and stable Discontinuous Galerkin methods for convection-diffusion problems", Preprint, URL: http://aam.mathematik.uni-freiburg.de/IAM/homepages/robertk/postscript/bdk_cdg2_preprint.pdf